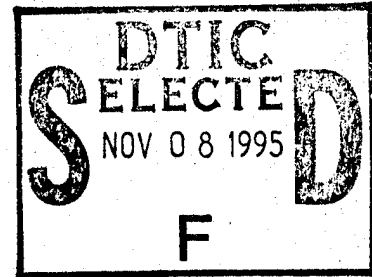


ADD 440773

NASA Contractor Report 178113



FINITE ELEMENT ANALYSIS OF END NOTCH FLEXURE SPECIMEN

(NASA-CR-178113) FINITE ELEMENT ANALYSIS OF N86-27429  
END NOTCH FLEXURE SPECIMEN Final Report  
(Missouri Univ.) 21 p HC A02/MF A01

CSSL 11D Unclas  
G3/24 43176

S. Mall and N. K. Kochhar

UNIVERSITY OF MISSOURI-ROLLA  
ROLLA, MISSOURI

DISTRIBUTION STATEMENT A  
Approved for public release  
Distribution Unlimited

GRANT NAG1-425  
May 1986

DEPARTMENT OF DEFENSE  
PLASTICS TECHNICAL EVALUATION CENTER  
ARRADCOM, DOVER, N. J. 07801

**NASA**  
National Aeronautics and  
Space Administration  
Langley Research Center  
Hampton, Virginia 23665

19951102 015

DTIC QUALITY INSPECTED 5

PLASTED  
50076

ABSTRACT

A finite element analysis of the end notch flexure specimen for mode II interlaminar fracture toughness measurement was conducted. The effect of friction between the crack faces and large deflection on the evaluation of  $G_{IIC}$  from this specimen were investigated. This analysis showed that the friction effect is negligible when crack length is greater than one-fourth of length of the specimen. Further, geometric nonlinear analysis is required to evaluate  $G_{IIC}$  when deflection is greater than the thickness of specimen.

Accession For	
NTIS CRA&I	<input checked="" type="checkbox"/>
DTIC TAB	<input type="checkbox"/>
Unannounced	<input type="checkbox"/>
Justification	
By <i>DTIC-AI memo</i>	
Distribution / <i>11-2-95</i>	
Availability Codes	
Dist	Avail and/or Special
<i>A-1</i>	

## INTRODUCTION

The delamination of laminated fiber reinforced composites is of current interest, particularly with regard to their durability and damage tolerance. It is the most commonly observed failure mode in composites. Fracture mechanics has been found to be a useful tool for understanding delamination [1]. Most of the work reported in this area has been concerned with the delamination in the opening mode, i.e. mode I. Delamination under shear sliding mode i.e. mode II and combined mode I-II situations are also the possible fracture modes of potentially greater significance in composite structures. Several studies on mixed-mode interlaminar fracture are also reported [1-4].

Recently attention has been given to mode II shear delamination [5-9]. Several investigators have used end notch flexure (ENF) specimen to measure shear mode strain energy release rate,  $G_{IIc}$ , for delamination growth [6-9]. This specimen is a beam with a crack (delamination) located on the neutral plane at one end and is subjected to the three-point bending. This specimen was initially utilized by Barrett and Foschi to measure Mode II critical-stress-intensity factor,  $K_{IIc}$ , for a strongly anisotropic fibrous material, wood [10]. Currently an ASTM task group is conducting a round robin test program using an end notch flexure specimen as a prelude to developing an ASTM standard for measurement of mode II interlaminar fracture toughness of composites. In this study, the end notch flexure specimen was analyzed using the finite element method for understanding its behavior and performance.

## FINITE ELEMENT ANALYSIS

The end notch flexure specimen geometry is shown in Fig. 1. Two geometries of the specimen were analyzed; (1) total length,  $2L = 7.62$  cm and (2)  $2L = 10.16$  cm. For both geometries, the thickness ( $2h$ ) of the specimen was taken equal to 0.30 cm which is nominal thickness of a 24 ply composite panel. These dimensions of  $L$  and  $h$  were selected since they were employed in experimental works [6,9]. The width of specimen was 2.54 cm. Only one material system was analyzed; unidirectional graphite/epoxy. The material properties used in finite element analysis are presented in Table 1.

A two-dimensional finite element program called GAMNAS [11] was used. A typical finite element mesh, shown in Fig. 2 consisted of about 1000 isoparametric four-node elements and had about 2400 degrees of freedom. The element size in the vicinity of the crack was  $0.02 \times 0.02$  mm in order to evaluate accurately the strain energy release rate  $G_{II}$ . This size was selected by previous experience [12] as well as by conducting the convergence test on  $G_{II}$  calculation with mesh refinement. The error in  $G_{II}$  obtained in the present study is estimated to be less than  $\pm 2\%$ . The strain energy release rate,  $G_{II}$ , in the analysis was computed using a virtual crack closure technique [13]. Plane-strain condition was assumed in the finite element analysis.

The analysis indicated that mode II deformation is achieved at the crack tip and that the accompanying mode I deformation causes closure and overlapping of the opposite faces of the crack. This is not possible physically. To prevent the overlapping of crack faces, the nodal coupling technique, available with GAMNAS program [11], was used. For this purpose, the multipoint constraint was applied at corresponding nodes to have the same displacements normal to the

crack faces. This resulted in pure mode II condition, i.e.  $G_I = 0$ . When the crack faces are pressed together as in this specimen, friction effects will occur. The friction effects on  $G_{II}$  calculation will be rather difficult to assess in the practical situation, however a reasonable estimate of its role can be investigated with the finite element analysis. The friction effect was modeled in the following manner. The analysis was conducted initially with the frictionless crack faces where displacements normal to the crack faces were matched at corresponding nodes. The normal reactions at the crack faces were obtained from this first step of calculation. The friction forces at the nodes on the crack faces were calculated for the assumed coefficient of friction. The finite element analysis of the specimen was conducted with these computed friction forces applied at the crack faces. This second step of analysis provided the new normal forces at the crack faces and corresponding friction forces. The analysis was repeated till the applied friction forces matched with the computed normal reactions. This required about two or three iterations.

## RESULTS AND DISCUSSIONS

### Comparison Between Theoretical and FEM $G_{II}$ Values

The measured compliance,  $c$ , versus crack length,  $a$ , relationship of a test specimen, in general, provides the most accurate evaluation of fracture toughness. However, it requires several measurements. On the other hand, fracture toughness can be measured from a single measurement of critical load if the necessary expression for  $G$  calculation is available. The experimental  $dc/da$  values were found to be subject to large errors due to small variation in compliance with crack length for small crack length values in the ENF specimen [7]. Therefore, the following expression for mode II strain energy release rate,  $G_{II}$  for this specimen was developed by Russell [7]:

$$G_{II} = \frac{9P^2 a^2}{16b^2 E_{11} h^3} \quad (1)$$

where  $P$ ,  $a$ ,  $b$ ,  $h$  are defined in Fig. 1 and  $E_{11}$  is the Young's modulus in longitudinal direction. The  $G_{II}$ , as expressed above, is based on a linear beam theory where shear deformation is neglected and the curvature

$$\frac{1}{R} = \frac{d^2 y/dx^2}{[1 + (dy/dx)^2]^{3/2}}$$

is approximated with  $1/R \simeq d^2 y/dx^2$ . The  $G_{II}$  values obtained from FEM analysis and from Eq.(1) for both geometries of the specimens; (1)  $2L = 7.62$  cm and (2)  $2L = 10.16$  cm, are compared for the normalized crack length,  $a/L$ , ranging from 0.125 to 0.9. The normalized crack length commonly used for measurement of  $G_{IIC}$  with this specimen was 0.5 [6,7,9]. Figure 3 shows that  $G_{IIC}$  from a linear beam theory,

i.e. from Eq.(1), is within 8% and 6% of its counterpart from FEM analysis for  $a/L = 0.5$  for specimens with  $2L = 7.62$  cm and  $2L = 10.16$  cm, respectively. Further, Fig. 3 shows that deviation between  $G_{II}$  from Eq.(1) and FEM analysis decreases with longer crack lengths and increases with shorter crack lengths. This comparison shows that the  $G_{IIC}$  should be evaluated from the end notch flexure specimen for  $a/L \geq 0.5$  if Eq.(1) is used.

#### Effect of Overhang Length

The effect of overhang length beyond the support was also investigated with finite element analysis. Specimens with overhang lengths of 6.35, 12.7 and 25.4 mm on each side were analyzed. The  $G_{II}$  values obtained for these cases were within  $\pm 1\%$  of each other. Thus, the overhang portion of this specimen has no effect in the evaluation of  $G_{IIC}$ .

#### Friction Effect

As mentioned previously, the friction was also modeled in FEM analysis. The most difficult task is to evaluate the actual coefficient of friction,  $\mu$ , between two pressed crack faces of ENF specimen. This was beyond the scope of the present study. However, a simple experiment was performed to estimate the coefficient of friction between two unidirectional graphite/epoxy laminates. This experiment involved the measurement of the force to initiate sliding between the two laminates with a known compressive load. The coefficient of friction,  $\mu$ , was found to be about 0.35. Therefore, the finite element analysis was conducted with the three values of  $\mu = 0.1, 0.3$  and  $0.5$  to understand the role of friction in a qualitative manner. Results of this analysis are shown in Fig. 4. Several observations can be made from

this analysis. For crack length commonly used in experimental investigation, i.e.  $a/L = 0.5$ , the effect of friction is negligible for all practical purposes if  $\mu$  is about 0.3. And, this effect is less in the ENF specimen with  $2L = 10.16$  cm in comparison to specimen with  $2L = 7.62$  cm. The friction effect shows a pronounced effect for shorter crack lengths and is negligible for longer crack lengths. This leads to an apparent conclusion that longer crack length should be employed for  $G_{IIC}$  evaluation, but this may cause the large deflection of specimen during testing and henceforth it may require the geometric nonlinear analysis as discussed later on.

The friction forces between the crack faces were primarily in the region above the support pin. Since it is always desirable to have the friction force as small as possible, it might, therefore, be preferable to use the shim or rollers between the crack face just above the support pin to reduce the coefficient of friction. Barrett and Foschi [10] suggested the use of roller between crack faces for measurement of  $K_{IIC}$  of wood from this type of specimen. However, it may not be convenient in composite specimens due to their small thicknesses.

#### Geometric Nonlinear Analysis

To investigate the effect of finite rotation due to large deflection, the geometric nonlinear analysis of the ENF specimen was conducted with the GAMNAS finite element program [11]. This analysis was conducted without friction. Figure 5 shows the comparison of  $G_{II}$  obtained from linear and geometric nonlinear analysis for both geometries of specimens for crack length  $a = 0.5L$ . Linear and nonlinear solution



are in agreement with each other up to deflection,  $\Delta$ , equal to the thickness of specimen,  $2h$ . For larger deflection, i.e.  $\Delta \geq 2h$ , the  $G_{II}$  would be overestimated from a linear analysis or Eq.(1). This overestimation depends on the deflection as shown in Fig. 5.

#### CONCLUDING REMARKS

A finite element analysis of the end notch flexure specimen for mode II interlaminar fracture toughness measurement was conducted. The effect of friction between the crack faces and large deflection on the evaluation of  $G_{IIC}$  from this specimen were investigated. Two geometries of the specimen, and one material system was studied. This study showed that this specimen should be preferably used for  $G_{IIC}$  measurement with crack length,  $a \geq 0.5L$  and deflection,  $\Delta \leq 2h$ .

#### ACKNOWLEDGEMENT

The work reported here was supported by NASA Langley Research Center, Hampton, VA and Weldon Spring Foundation, University of Missouri. The authors wish to acknowledge the support and encouragement of Dr. W. S. Johnson, NASA Langley Research center during the course of this investigation.

## REFERENCES

1. O'Brien, T.K., "Interlaminar Fracture of Composites", NASA TM 85768, June 1984.
2. Wilkins, D.J., Eisenmann, J.R., Camin, R.A., Margolis, W.S. and Benson, R.A., "Characterizing Delamination Growth in Graphite-Epoxy", Damage in Composite Materials: Basic Mechanisms, Accumulation, Tolerance, Characterization, ASTM STP 775, American Soc. for Testing and Materials, 1982, pp. 168-183.
3. Ramkumar, R.L. and Whitcomb, J.D., "Characterization of Mode I and Mixed-Mode Delamination Growth", Delamination and Debonding of Materials, ASTM, STP 876, American Society for Testing and Materials, Philadelphia, 1985, pp. 315-335.
4. Armanios, E.A., Rehfield, L.W., and Reddy, A.D., "Design Analysis and Testing for Mixed-Mode and Mode II Interlaminar Fracture of Composites" Composite Materials: Testing and Design (Seventh Conference), ASTM STP 893, American Society for Testing and Materials, Philadelphia, 1986, pp. 232-255.
5. Chatterjee, S.N., Pipes, R.B. and Blake, R.A., Jr., "Criticality of Disbonds in Laminated Composites", Effects of Defects in Composite Materials, ASTM, STP 836, American Society for Testing and Materials, Philadelphia, 1984, pp. 161-174.
6. Russell, A.J. and Street, K.N., "Moisture and Temperature Effects on the Mixed-Mode Delamination Fracture of Unidirectional Graphite Epoxy", Delamination and Debonding of Materials, ASTM, STP 876, American Society for Testing and Materials, Philadelphia, 1985, pp. 349-370.
7. Russell, A.J., "Factors Affecting the Interlaminar Fracture Energy of Graphite/Epoxy Laminates", Progress in Science and Engineering of Composites; Proceedings of ICCM-IV, Tokyo, 1982, pp. 279-286.
8. Giare, G.S., "Fracture Toughness of Unidirectional Fibre Reinforced Composites in Mode II", Engineering Fracture Mechanics, Vol. 20, No. 1, pp. 11-21, 1984.
9. Murri, G.B. and O'Brien, T.K., "Interlaminar  $G_{IIC}$  Evaluation of Toughened-Resin Matrix Composite Using the End-Notched Flexure Test", AIAA Paper No. 85-0647, Proceedings of the 26th AIAA/ASME/ASCE/AHS Structures, Structural Dynamics and Materials Conference, April 15-17, 1985, Orlando, FL.
10. Barrett, J.D. and Foschi, R.O., "Mode II Stress-Intensity Factors for Cracked Wood Beams", Engineering Fracture Mechanics, Vol. 9, pp. 371-378, 1977.

11. Whitcomb, J.D. and Dattaguru, B., "User's Manual for GAMNAS-- Geometric and Material Nonlinear Analysis of Structures", NASA TM 85734, Jan. 1984.
12. Mall, S., Johnson, W.S., and Everett, R.A., Jr., "Cyclic Debonding of Adhesively Bonded Composites", Adhesive Joints: Their Formation, Characteristics, and Testing, K. L. Mittal, Ed; Plenum Press, New York, 1984, pp. 639-658.
13. Rybicki, E.F. and Kanninen, M.F., "A Finite Element Calculation of Stress Intensity Factors by a Modified Crack Closure Integral", Engineering Fracture Mechanics, Vol. 9, No. 4, 1977, pp. 931-938.

TABLE 1 - GRAPHITE/EPOXY MATERIAL PROPERTIES<sup>a</sup>

Modulus <sup>b</sup> , GPa			Poisson's Ratio <sup>b</sup>	
$E_{11}$	$E_{22}$	$G_{12}$	$\nu_{12}$	$\nu_{23}$
131.0	13.0	6.4	0.34	0.35

a:  $E_{33} = E_{22}$ ,  $\nu_{13} = \nu_{12}$ ,  $G_{13} = G_{12}$

b: The subscripts 1, 2 and 3 correspond to the longitudinal, transverse, and thickness directions, respectively, of a unidirectional ply.

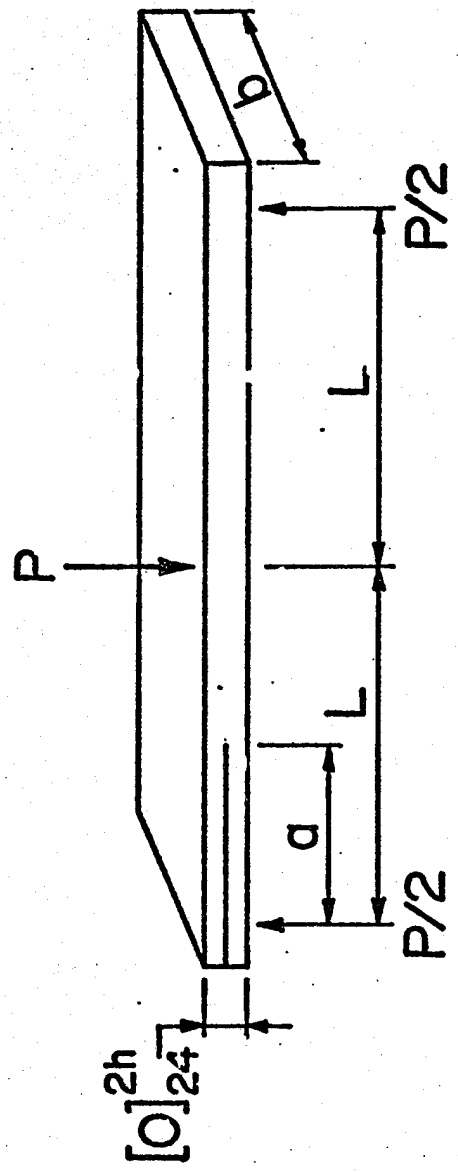


Fig. 1. End Notch Flexure Specimen

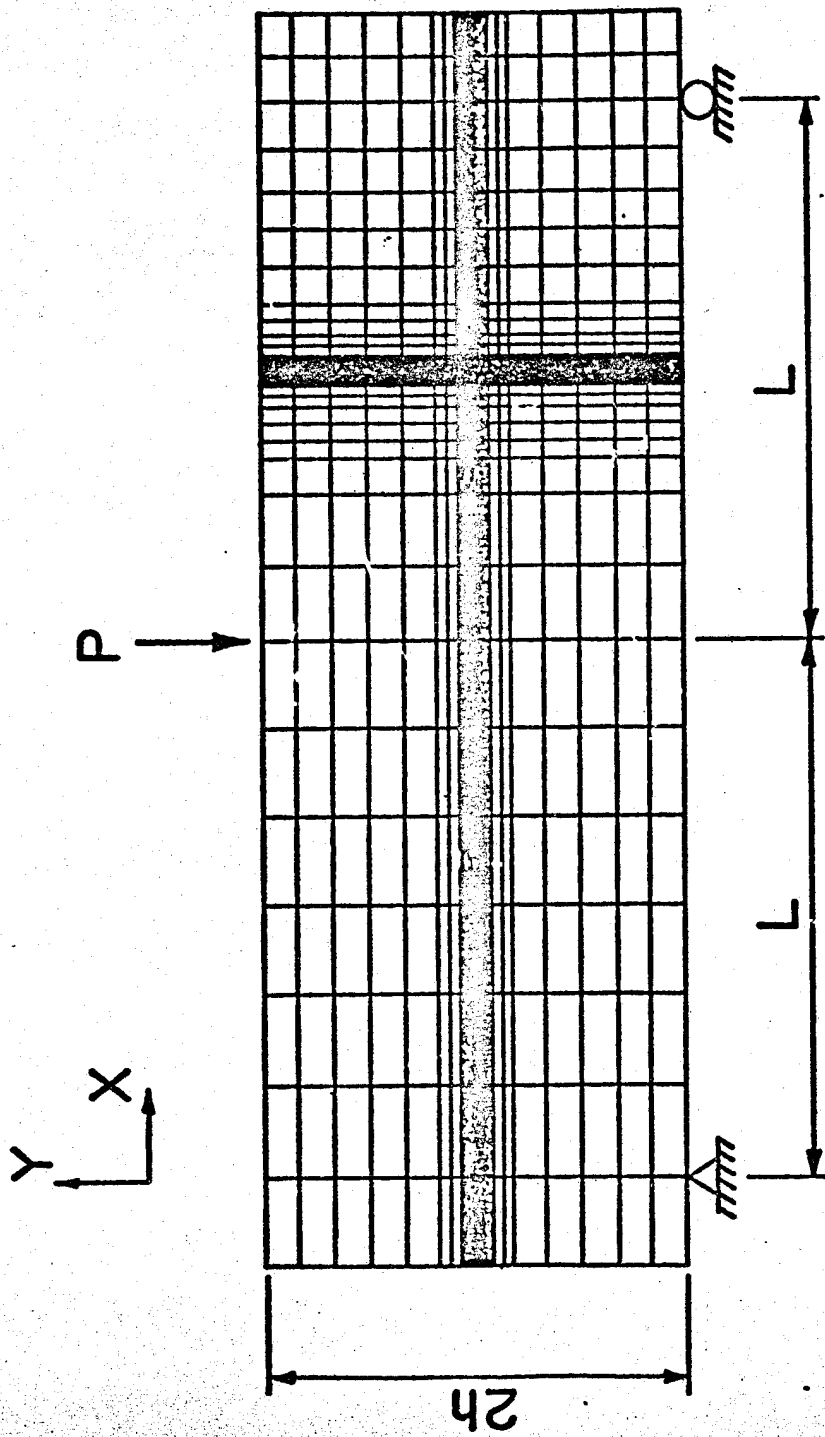


Fig. 2. Finite Element Mesh (Y Coordinates are magnified 10X)

$$\frac{G_{II}^{FEM}}{G_{II}^{Th}}$$

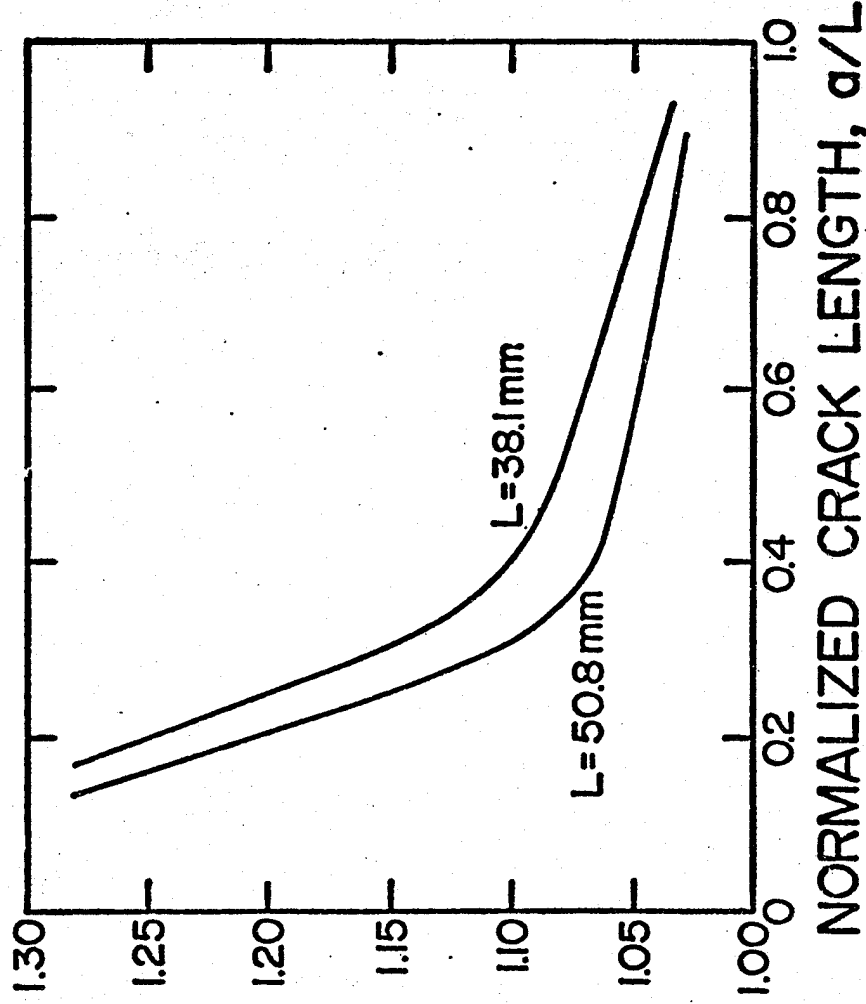
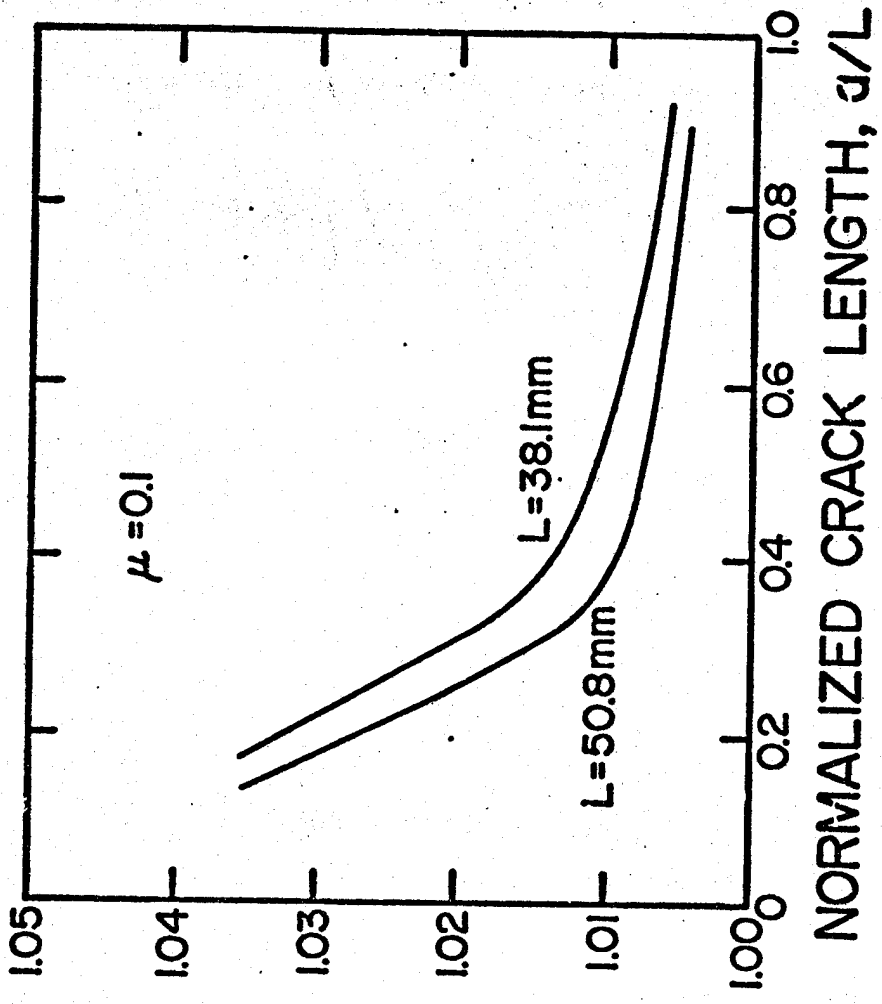


Fig. 3. Ratio of  $G_{II}$  from FEM analysis to  $G_{II}$  from Eq. (1) as a function of normalized crack length.





$$\frac{G_{II}^{FEM}(\mu=0.1)}{G_{II}^{FEM}(\mu=0)}$$

Fig. 4 (a). Ratio of  $G_{II}$  with  $\mu = 0.0$  to  $G_{II}$  with  $\mu = 0.1$  from FEM analysis as a function of normalized crack length.

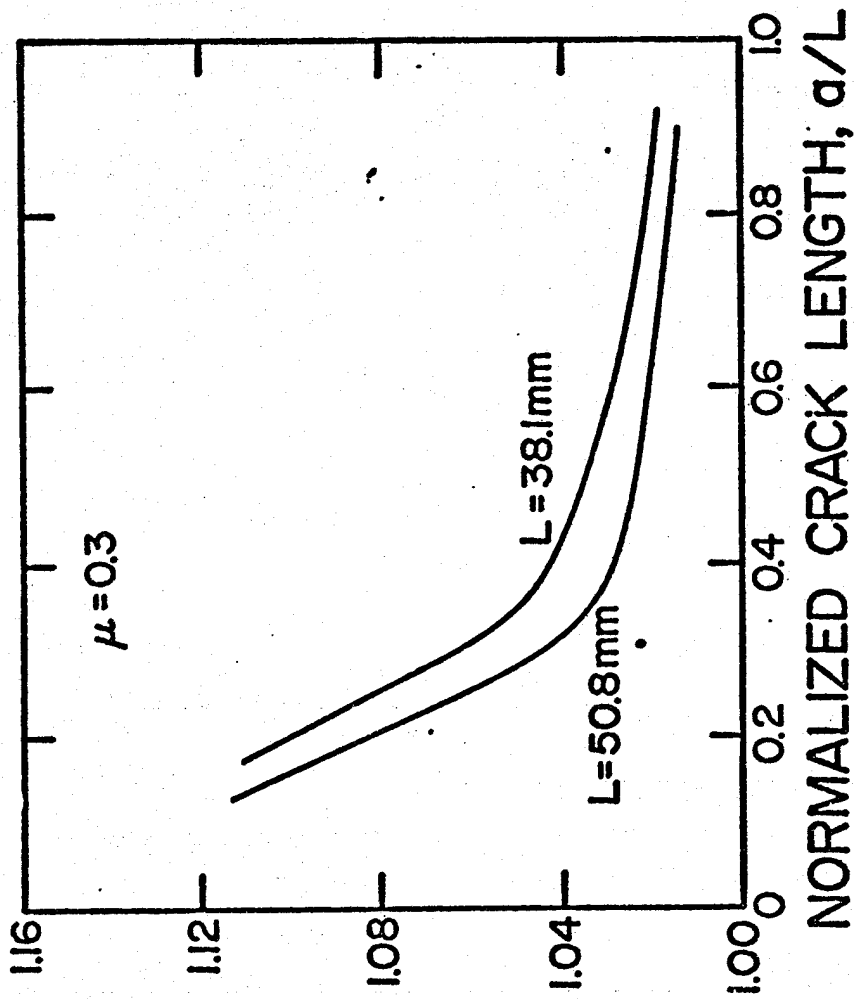


Fig. 4 (b). Ratio of  $G_{II}$  with  $\mu = 0.0$  to  $G_{II}$  with  $\mu = 0.3$  from FEM analysis as a function of normalized crack length.

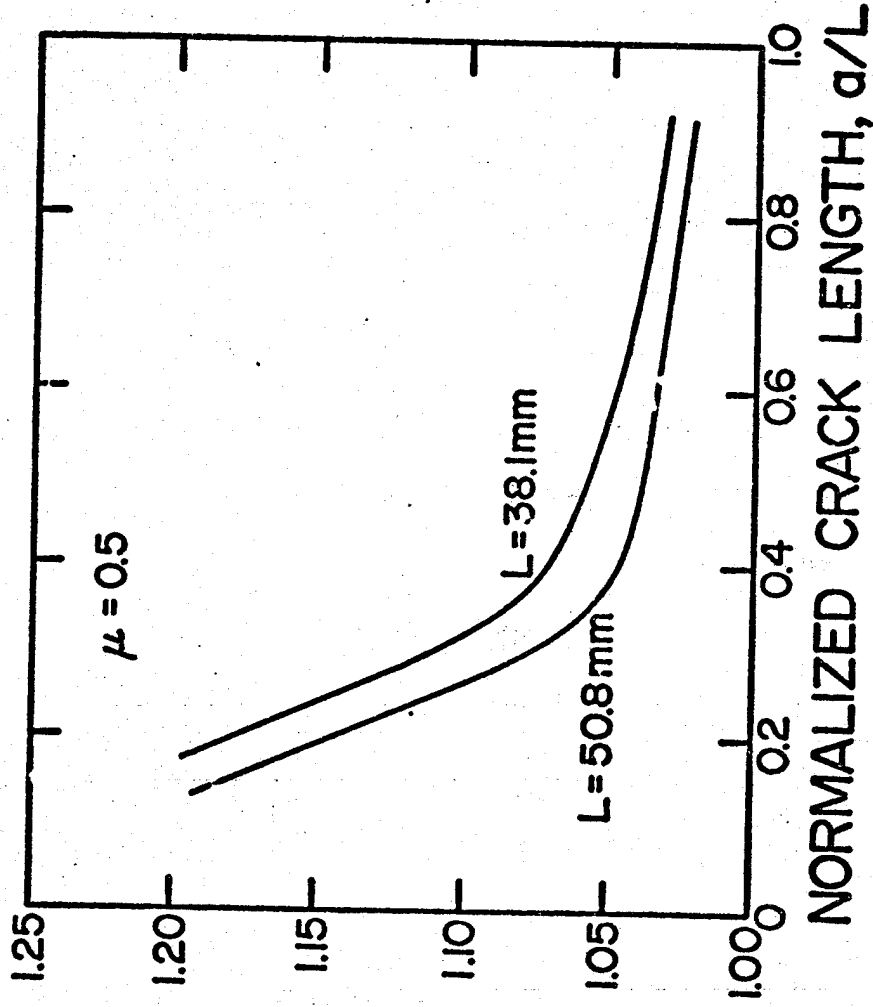


Fig. 4 (c). Ratio of  $G_{II}$  with  $\mu = 0.0$  to  $G_{II}$  with  $\mu = 0.5$  from FEM analysis as a function of normalized crack length.

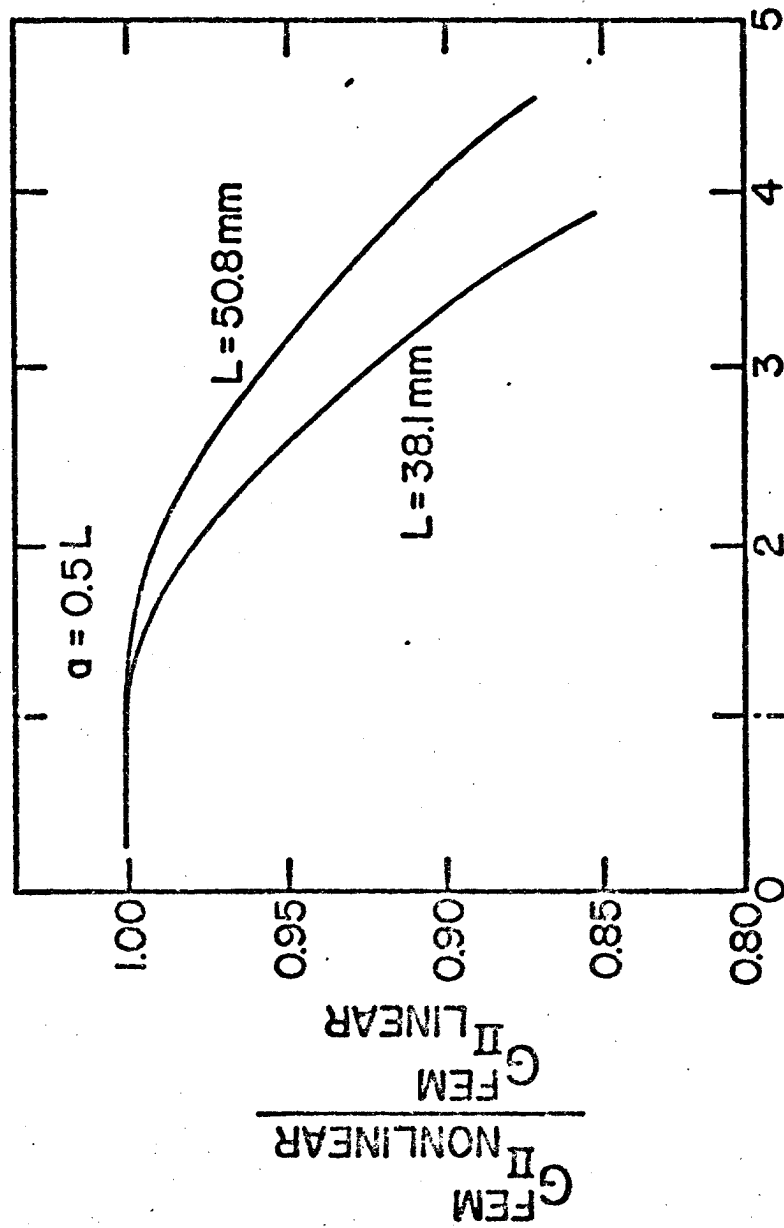


Fig. 5. Ratio of  $G_{II}$  from nonlinear analysis to  $G_{II}$  from linear analysis as a function of normalized deflection.

Standard Bibliographic Page

1. Report No. NASA CR-178113		2. Government Accession No.		3. Recipient's Catalog No.	
4. Title and Subtitle FINITE ELEMENT ANALYSIS OF END NOTCH FLEXURE SPECIMEN				5. Report Date May 1986	
				6. Performing Organization Code	
7. Author(s) S. Mall and N. K. Kochhar				8. Performing Organization Report No.	
				10. Work Unit No.	
9. Performing Organization Name and Address University of Missouri-Rolla Department of Engineering Mechanics Rolla, MO 05401 M3949516				11. Contract or Grant No. NAG1-425	
				13. Type of Report and Period Covered Contractor Report	
12. Sponsoring Agency Name and Address National Aeronautics and Space Administration Washington, DC 20546				14. Sponsoring Agency Code 534-06-23-03	
				15. Supplementary Notes Langley Technical Monitor: Dr. W. S. Johnson Final Report	
16. Abstract A finite element analysis of the end notch flexure specimen for mode II interlaminar fracture toughness measurement was conducted. The effect of friction between the crack faces and large deflection on the evaluation of $G_{IIC}$ from this specimen were investigated. Results of this study are presented in this paper.					
17. Key Words (Suggested by Authors(s)) Interlaminar fracture toughness Mode-II delamination End notch flexure specimen				18. Distribution Statement  Unclassified-Unlimited  Subject Category 24	
19. Security Classif.(of this report) Unclassified		20. Security Classif.(of this page) Unclassified		21. No. of Pages 20	22. Price A02

For sale by the National Technical Information Service, Springfield, Virginia 22161